Original Research Article

THERMAL AND STRUCTURAL CHARACTERIZATION OF COKE DEPOSITION ON SPENT NiMo CATALYST USED DURING CATALYTIC UPGRADING OF HEAVY OIL

ABSTRACT

Catalyst deactivation has become a major concern in the refining industry globally. The deactivation of hydroprocessing catalyst by coke deposition reduces its useful life, the on-stream time of the process involved and the profitability of upgrading heavy oils to useful products. There are various methods used in thermal and structural characterization but for the purpose of this research journal, Thermogravimetric Analysis (TGA), Scanning Electron Microscopy (SEM), X-Ray Diffraction (XRD) and Fourier Transform Infrared (FTIR) were carried out on both fresh and spent NiMo catalyst. The TGA results of the spent catalyst samples indicates the presence of coke species with the major portion of the species being 'medium' and 'hard' coke (second and third stage). There was also no significant change in loss of weight with change in heating rate. In comparison to the fresh catalyst, the SEM micrograph of the used catalyst indicates the formation of poor porous-structure and block-shaped crystallites depicting the sintering of particles because of the higher calcinationtemperature. O–C–O bond stretching vibrations with an anatase morphology were observed using FTIR on the spent catalyst sample confirming the presence of the coke species while the XRD results showed the formation and nature of carbonaceous deposits on the spent catalyst's surfaces. A rutile phase with a tetragonal symmetry was detected for spent NiMo diffraction peaks, with the major phase indicating the presence of Carbon with a hexagonal phase.

Keywords: Catalyst, coke, NiMo, characterization, heavy oil, TGA, FTIR, SEM, XRD, hydroprocessing, catalyst deactivation.

1. INTRODUCTION

Thermal cracking was previously used in upgrading heavy oil in refineries before catalytic cracking came into use as a more desirable process because of two major reasons. Catalytic cracking minimizes the yield of other products and maximizes the yield of gasoline (Sundaram, 2017). The gasoline produced by catalytic cracking is of higher quality and this is due to the various reactions that take place in the reactor during catalytic cracking. In recent years, hydroprocessing catalysts have been widely accepted and highly

preferred in the refining industry due to many reasons. One of the reasons is the result attained in the purification of different petroleum streams particularly in the catalytic upgrading of heavy oils and residues. These catalysts have also provided a very wide range of well-proven products for a wide range of hydrodesulphurization (HDS) and hydrodenitrogenation (HDN) duties. Catalysts usually used in residue hydrotreating processing consists of Molybdenum (Mo) and prompter Nickel (Ni) or Cobalt (Co) on alumina support to increase the removal of various unwanted impurities such as Nitrogen, Sulphur and metals as a result of hydrodenitrogenation, hydrodesulphurization and hydrodemetallization reactions (Zahranet al., 2020).

Catalysts are mainly used to enhance the efficiency of catalytic cracking and maximize the removal and reduction of polyaromatic content by breaking heavier hydrocarbons with higher boiling points to short-chain hydrocarbons with lower boiling points that can even be further processed in other units within the refinery (Ihediwa, 2021). In the catalytic upgrading of heavy oils, NiMo catalyst stands out as a result of its high desulphurization activity for reducing polyaromatic compounds of gas oil and is also remarkable, without decreasing the oil content by overcracking.

A serious issue concerning the cost and process of upgrading heavy oils arises from the deactivation of catalyst. Reactions involving the catalytic upgrading of heavy oils are likely to produce solid carbonaceous deposits, widely referred to as ‘coke’ (Dim et al., 2014). The deposition of coke on fresh catalyst results in the deactivation of the catalyst which reduces its useful life. The profitability of a catalytic process isdependent on the catalyst’s lifetime hence these catalysts have to be regenerated before they can be used again (Hart, 2014). The characterization of coke on spent catalyst has become of very significant interest as catalyst deactivation has become a major concern in the refining industry (Daligauxet al., 2022). Catalyst deactivation occurs as a result of basically two reasons which are metal deposition and coke formation and deposition. Other causes of catalyst deactivation include poisoning, fouling, sintering as well as chemical and thermal degradation.Deactivation has been found out to be dependent on the nature of the feed and its composition, process parameters and reactor design. The rate of deactivation is also faster when the heavy oil that is to be upgraded has high content of asphaltenes and metals (Maity et al., 2012). Coking in catalytic upgrading of heavy oil presents a challenge in that it occurs in side reactions to the main reaction and, therefore, in contrast to poisoning, fouling and other causes of catalyst activation, which can be controlled and minimized by improving feed purification and better control of operating condition respectively, coking cannot be completely eliminated.Due to the industrial importance of the catalytic cracking of heavy oils, many articles have been published on the process and on the characterization of coke deposition on spent catalyst in order to understand the coking behavior, influence of process parameters and feed composition

on catalyst deactivation and to obtain relevant information on the structure and composition of coke formed and deposited during the catalytic upgrading of heavy oils.

This research work is aimed at thermally and structurally characterizing coke deposition on NiMo catalyst used in catalytic upgrading of heavy oil. The thermal characterization of coke was carried out using thermogravimetric analysis (TGA) to find out its thermal stability and the fraction of volatile components by monitoring the weight change that occurs as the coke sample was heated by gradually raising the temperature of a sample in a furnace as weight is measured at a constant rate (2.5, 5.0 and 15 □/min respectively). Structural characterization was carried out using three methods which are Scanning Electron Microscopy (SEM), X-Ray Diffraction (XRD) and Fourier Transform Infrared (FTIR).

SEM is used to characterize the morphology of the formed-coke deposited at the outer layer of the catalyst pellet as well as the crystalline structure and orientation of materials making up the catalyst sample. X-ray diffusion is a technique that provides detailed information about the crystallographic structure and physical properties of materials. The physicochemical properties and microstructure of spent NiMo catalyst are characterized by X-ray diffraction to determine type of crystal and crystallinity of the spent catalyst. FTIR is carried out to ascertain the nature of the coke species that were extracted from the spent catalyst. It is used for characterizing the morphology of the sample and detecting the types of functional groups of the formed-coke on the sample. Characterizing coke deposition helps to identify the nature, location, structure and composition of coking material which is very essential for designing of improved and commercially viable catalysts.

The contribution and strength of this research lie in its integrated approach to characterizing coke deposition on NiMo catalysts used in heavy oil upgrading, offering both thermal and structural insights that are valuable for catalyst design and refining processes. While previous studies have focused on individual aspects of coke characterization, this study combines thermogravimetric analysis (TGA), X-ray diffraction (XRD), Fourier-transform infrared spectroscopy (FTIR), and scanning electron microscopy (SEM) to comprehensively examine both fresh and spent catalysts.

2. MATERIAL AND METHODS

Fresh Catalyst Properties

The used catalyst studied in this work is a commercial sample of Ketjenfine hydro-processing catalyst Nickel-Molybdenum (NiMo) (Extrudates) from United States (US). The composition and properties of catalysts studied as specified are Precipitated silica: < 10; Nickel (II) oxide: < 10; Molybdenum (VI) oxide:

< 30; Phosphorus pentoxide: 0-9; Aluminum oxide: balance (w/w%) of particles with diameter ~1mm and with a length of ~7mm, color is yellow, melting point is greater than 800°C, bulk density is 550 - 950 kg m-3 and odorless. The spent catalyst is the reaction product of Canadian heavy oil in a Micro-reactor in presence of nitrogen gas at 425 °C, 20 bars for 8 hours.

2.1 The Fourier Transform Infrared Spectroscopy (FTIR)

Fourier transform infrared spectroscopy (FT-IR) analysis was performed for all samples isolated to have a prompt result regarding the bio mineral. A few crystals were mixed with KBr (Merck for spectroscopy) and pulverized in an agate mortar to form a homogenous powder from which, under a pressure of 7 tons, the appropriate pellet was prepared. All spectra were recorded from 4000 to 400 cm-1 using the Pelkin Elmer 3000 MX spectrometer. Scans were 32per spectrum with a resolution of 4 cm1.The IR spectra were analyzed using the spectroscopic software Win-IR Pro Version 3.0 with a peak sensitivity of 2cm-1. The data was analyzed on computer system and the result presented in a graphical form.

2.2 Thermo-gravimetry Analysis (TGA)

Thermo-gravimetric analysis (TGA) is an analytical technique where the weight of a sample is measured over time, as the temperature changes while heating. Typical weight loss profiles are analyzed to obtain the amount or percent of weight loss at any given temperature and the amount or percent of non-combusted residue at final temperature, and the temperature of various degradation steps. The analysis was carried out for each sample in a thermal gravimetric analyzer SDT Q600 V8.3. Gas flow and pressure were controlled by a pressure/flow controller. Time (min), weight (mg), heat flow (mW), temperature (°C) and temperature difference (°C) data were acquired at defined intervals and the data stored on the computer's hard disk. The analysis was carried out at 3 different heating rates (2.5, 5 and 15 °C/min respectively). The temperature range for heating was between 25 to 1005(°C) for each sample and the flow rate of nitrogen used was 20.0 ml/min. Data from thermo-gravimetric analysis was analyzed on computer system and shown by a graph representing weight % as a function of temperature.

2.3 Scanning Electron Microscopy (SEM)

All samples must be of an appropriate size to fit in the specimen chamber and are generally mounted rigidly on a specimen holder called a specimen stub. Several models of SEM can examine any part of a 6-inch (15

cm) semiconductor wafer, and some can tilt an object of that size to 45^{o}.Samples were coated with platinum coating of electrically conducting material, deposited on the sample either by low-vacuum sputter coating or by high-vacuum evaporation. SEM instruments place the specimen in a relative high-pressure chamber where the working distance is short and the electron optical column is differentially pumped to keep vacuum adequately low at the electron gun. The high-pressure region around the sample in the ESEM neutralizes charge and provides an amplification of the secondary electron signal.The SEM of the fresh catalyst was carried out at 5, 10 and 20 µm while that of the spent catalyst was carried out at 5, 20 and 50 µm.

2.4 X-ray diffraction (XRD)

Powdered samples were pelletized and sieved to 0.074mm. These were later taken in an aluminum alloy grid (35mm x 50mm) on a flat glass plate and covered with a paper. Wearing hand gloves, the samples were compacted by gently pressing them with the hand. Each sample was run through the Rigaku D/Max-lllC X-ray diffractometer developed by the Rigaku Int. Corp. Tokyo, Japan and set to produce diffractions at scanning rate of 2^{o}/min in the 2 to 50^{o} at room temperature with a CuKa (Copper K-α: an x-ray energy frequently used in x-ray lab scale equipment) radiation set at 40kV and 20mA. The diffraction data (d value and relative intensity) obtained was compared to that of the standard data of minerals from the mineral powder diffraction file, ICDD which contained and includes the standard data of more than 3000 minerals.

3. RESULT AND DISCUSSION

3.1 TGA

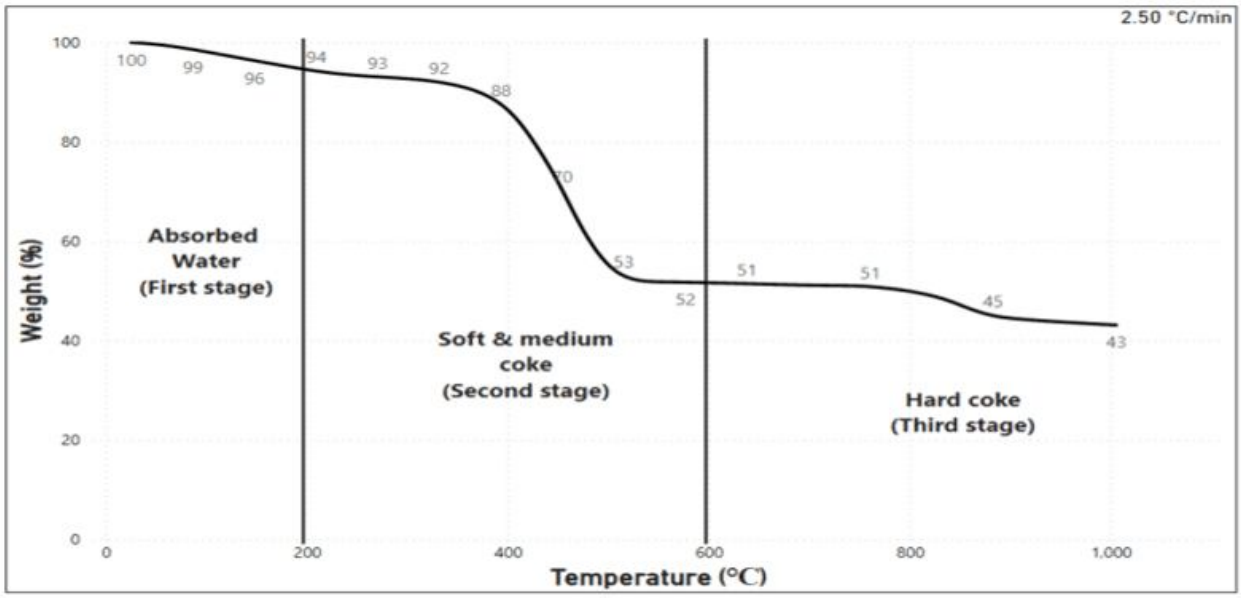

Figure 1.TGA profile of the spent NiMo catalyst at 2.50 □/min

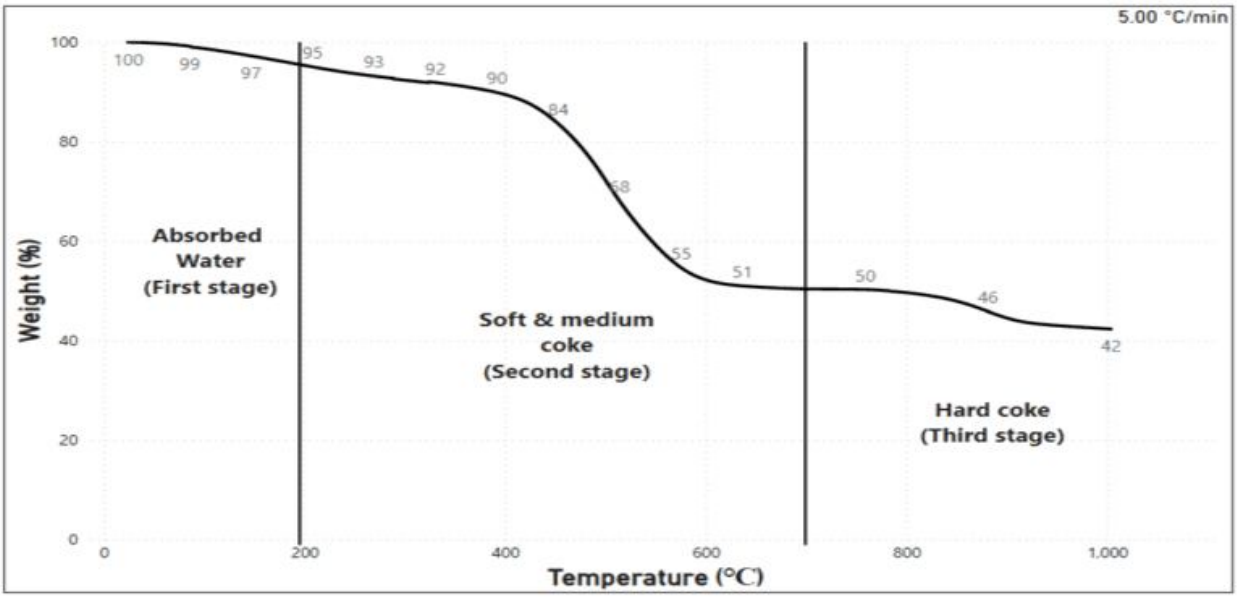

Figure 2.TGA profile of the spent NiMo catalyst at 5.00 □/min

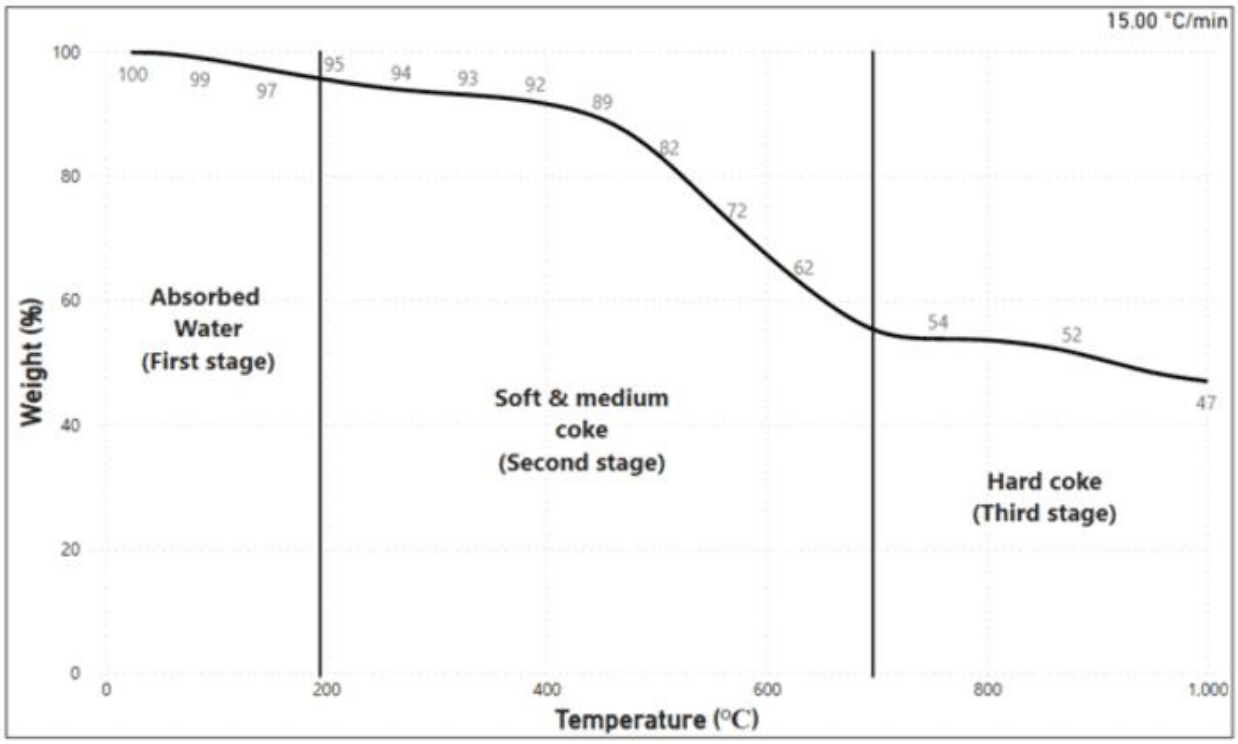

Figure 3.TGA profile of the spent NiMo catalyst at 15.00 □/min

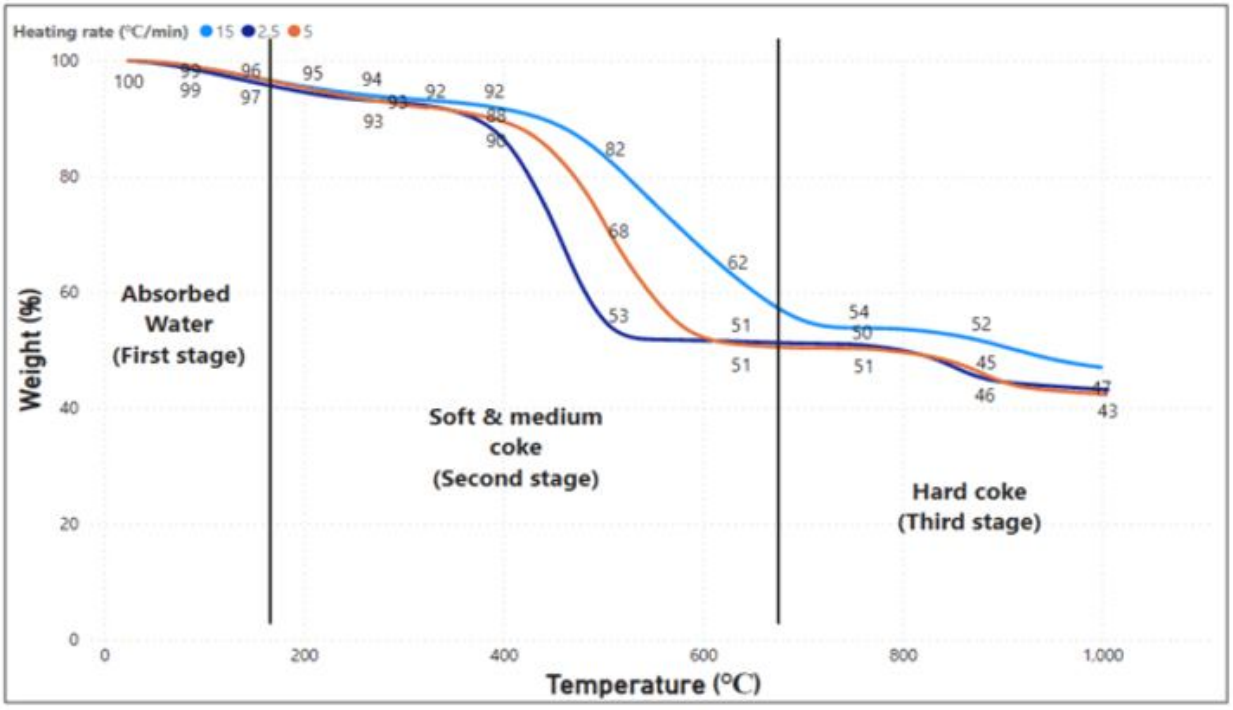

Figure 4.TGA profile of the spent NiMo catalyst at 2.50, 5.00 and 15.00 □/min (colored image*)

In this study, the total carbon deposited on the spent catalyst was investigated using TGA. Figures 1, 2 and 3 shows the TGA graphs for heating rates of 2.50, 5.00 and 15.00 □/min respectively and a constant Nitrogen flow rate of 20.0 ml/min while figure 4 is a TGA graph showing the weight losses of the 3 heating rates for comparison as well as the removal of volatile matter in the samples.

It was observed that as the temperature gradually increased for all samples, there was a continuous reduction in the weight of the spent catalyst. It was evident that the thermal decomposition of the samples had three different stages. TGA results indicated that the first weight loss in the range of 25-200°C signifies the presence of bonded water molecules and the dehydration of the moisture in the sample. It is also attributed to soft coke (light organic compounds present) desorption. The second weight loss stage occurred between 200-700°C and is attributed to the removal of soft and medium coke. The third weight loss stage occurred between 700-1005°C and is attributed to the removal of hard coke which decomposes slowly and is evident in the graphs.

Evidently, varying the heating rate (2.50 to15.00 °C/min) did not affect the mass loss significantly. The total mass loss at 2.50 °C/min was about 57% whereas that at 15.00 °C/min was 53%. Generally, difference in mass loss could be due to fact that more energy was added at the latter condition than at the beginning of the heating process.

3.2 X-ray Diffraction (XRD)

The X-ray Diffraction (XRD) measurements were performed on Catalyst powders using a diffractometer (BrukerAxs D8 Advance, Germany). CuKαradiation (λ= 1.54˚A) was used at a voltage of 40 kV and a current of 25 mA.

Sample	: Fresh Nimo	File : Sg2～1.ASC	Date : Feb 16 7:30:24	Operator :
Comment	: Qualitative	Memo		
Method	: 2nd differential	Typica width : 0.065 deg.	Min. Height	5000:00 c p s

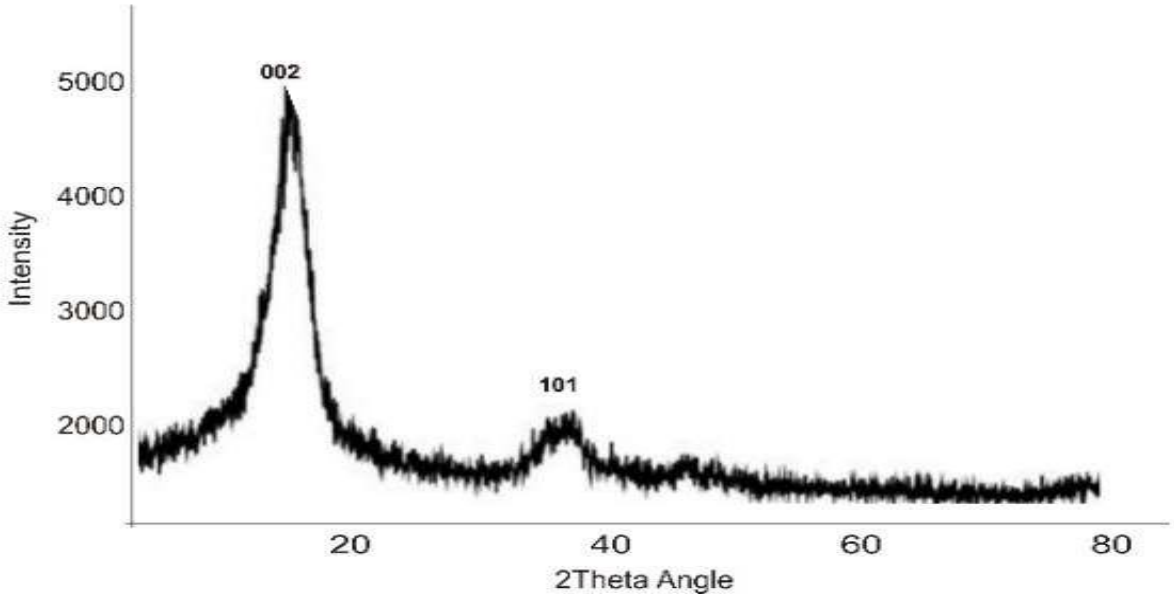

Figure 5.XRD analysis of fresh NiMo

Sample	: Spent NiMo	File : Sg2～1.ASC	Date : Feb 16 15:35:20	Operator :
Comment	: Qualitative	Memo		
Method	: 2nd differential	Typica width : 0.065 deg.	Min. Height	130:00 c p s

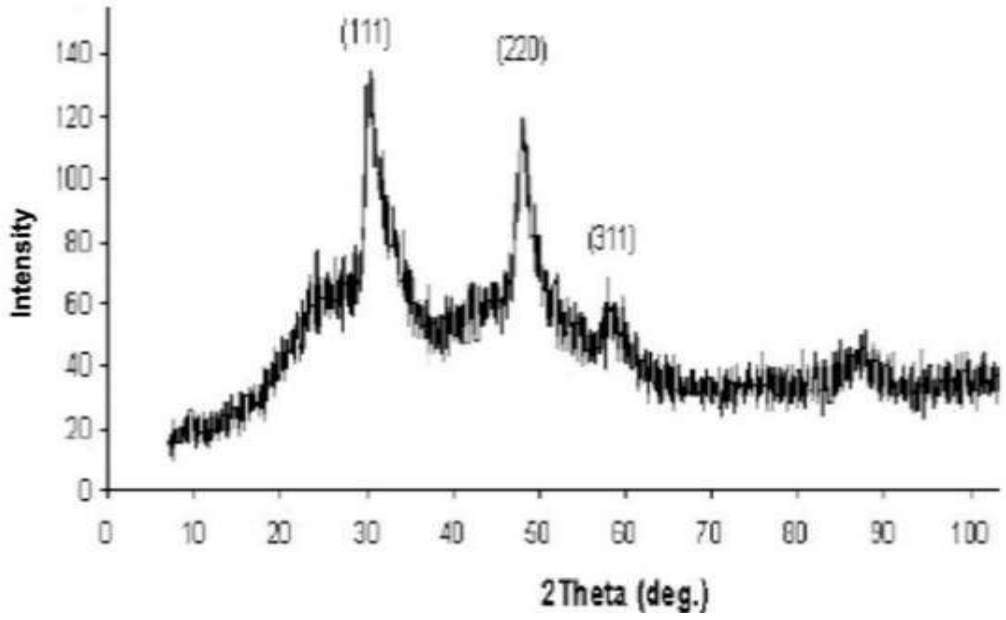

Figure 6.XRD analysis of Spent NiMo

The XRD spectra for both fresh and spent NiMo catalyst samples reveal critical structural transformations that shed light on the catalyst's deactivation mechanism during heavy oil upgrading. For the fresh NiMo catalyst, the dominant peak at 36.7° with the Miller index (311), a d-spacing of 0.244 nm, and space group 227:Fd3m, indicates a spinel phase. This structure is typical of NiMo catalysts in their active state, where the Ni and Mo species are highly ordered and available for catalytic activity. Additional peaks at 31.74° and 44.63°, corresponding to the (220) and (400) planes, respectively, further confirm the spinel structure, highlighting a well-defined cubic lattice that is known to enhance catalytic efficacy in hydrodesulphurization (HDS) and hydrodenitrogenation (HDN) processes. This characterization provides a standard for assessing structural integrity before exposure to upgrading conditions. In contrast, the XRD pattern of the spent NiMo catalyst reveals important structural evolution, likely resulting from prolonged exposure to high temperatures and coke formation. A significant shift is observed, with the emergence of a rutile phase exhibiting tetragonal symmetry. The major diffraction peak for this phase appears at 54.32° with a (211) plane and a reduced d-spacing of 0.16 nm. This phase transformation suggests structural reorganization in the catalyst due to the cumulative effects of coke deposition, which may limit the mobility of Ni and Mo species, diminishing catalytic activity. Peaks observed at 31.2° and 36.8°, corresponding to planes (220) and (311) with the space group 227:Fd3m, indicate partial retention of the original cubic phase. However, the intensity and broadening of these peaks suggest lattice strain and possible sintering effects, contributing to a decrease in catalyst surface area and active site availability. The development of a new peak at 32.8°, indexed to the (104) plane with a d-spacing of 0.27 nm, reveals the presence of carbon in a hexagonal phase, confirming significant coke deposition on the catalyst surface. This accumulation of coke is known to occlude active sites and hinder reactant access, leading to a decline in catalytic efficiency. The structural changes documented here, particularly the transition from a spinel to a rutile phase and the presence of carbon deposits—underscore the influence of coke and metal deposition on catalyst deactivation.

3.3 FTIR Analysis

The FTIR analysis of the prepared fresh and spent NiMo catalyst samples are shown in Figure 7 and.8 respectively. The FTIR spectra provide key insights into the structural evolution and deactivation of the NiMo catalyst during heavy oil upgrading. For the fresh NiMo catalyst, a strong peak at 912 cm^{-1} corresponds to Ni–Mo stretching vibrations, indicating a stable spinel structure essential for catalytic efficiency. However, in the spent catalyst, the peak shifts to 900 cm^{-1}, suggesting changes in the NiMo

bonding environment likely due to coke formation and metal sintering effects. The appearance of a new peak at 744 cm^{-1}, linked to O–C–O stretching vibrations, signifies an anatase-phase TiO_2 morphology. This transition is consistent with the anatase crystal vibration range (500–800 cm^{-1}) and reflects structural alteration from prolonged high-temperature exposure.The small peak around 850 cm^{-1}, also associated with O–C–O bonds, implies CO formation, hinting at partial oxidation of carbonaceous deposits on the catalyst. Additionally, a peak shift below 700 cm^{-1}, attributed to C–O stretching, further supports the presence of coke deposits and changes in the catalyst surface chemistry. These spectral shifts indicate significant structural reorganization and carbon deposition, both of which play critical roles in catalyst deactivation by reducing active sites and altering the catalyst's crystallographic framework.

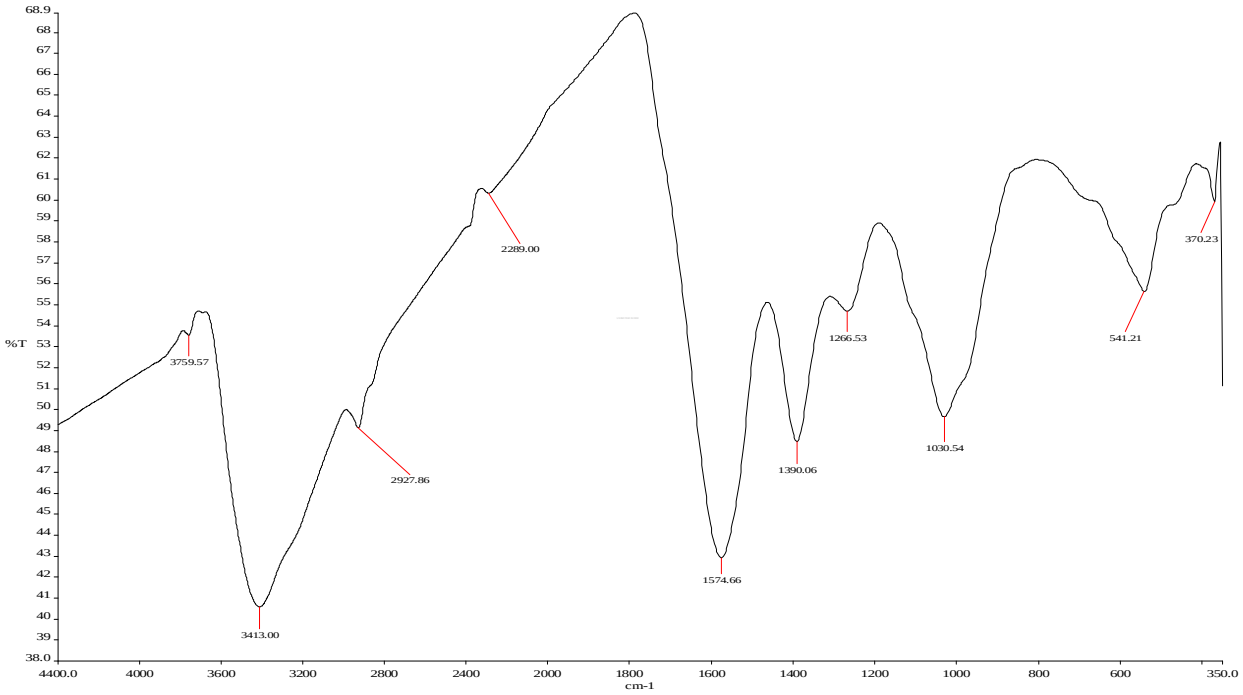

Figure 7.FTIR analysis of fresh NiMo catalyst

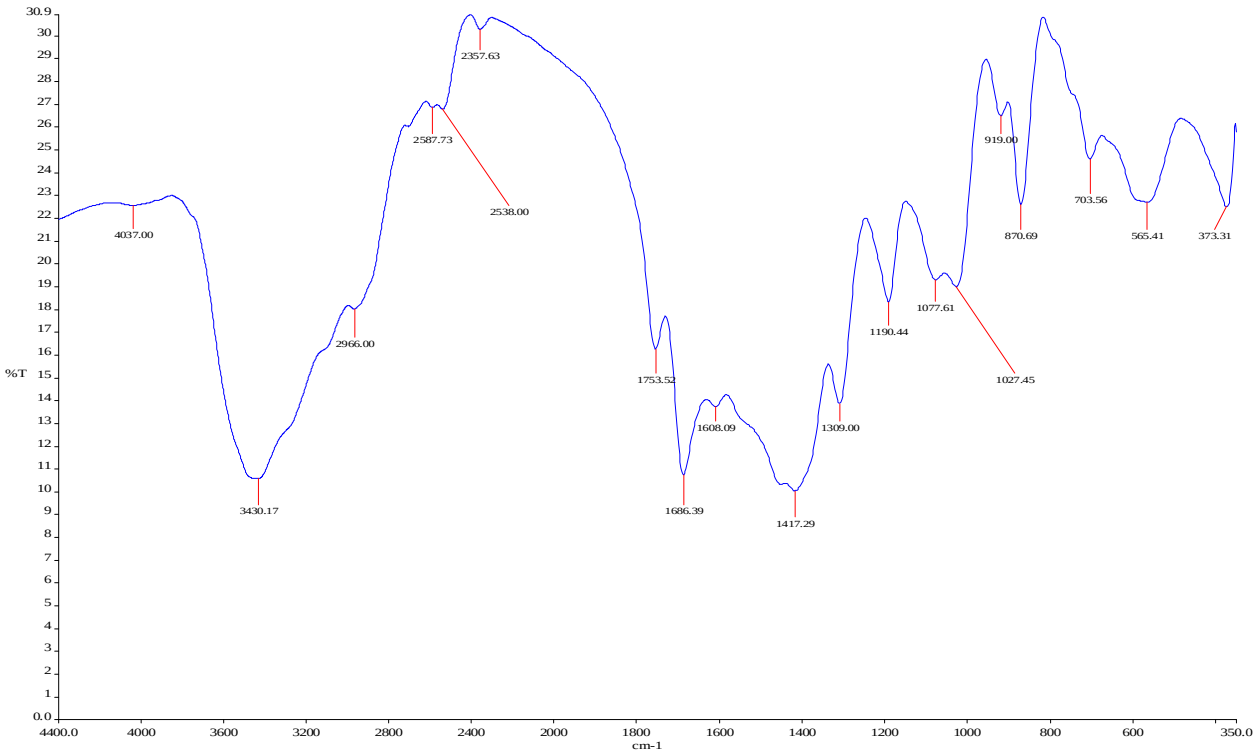

Figure 8.FTIR analysis of spent NiMo catalyst

3.4 SEM Analysis

Scanning electron microscopy analysis was used to investigate the morphology of the surface of the catalyst samples. The surface topography of the pure catalyst powder was characterized using Scanning Electron Microscopy (JSM-7600F JEOL, SEM, Japan) at an accelerating voltage of 20 kV and a working distance of 10 m.

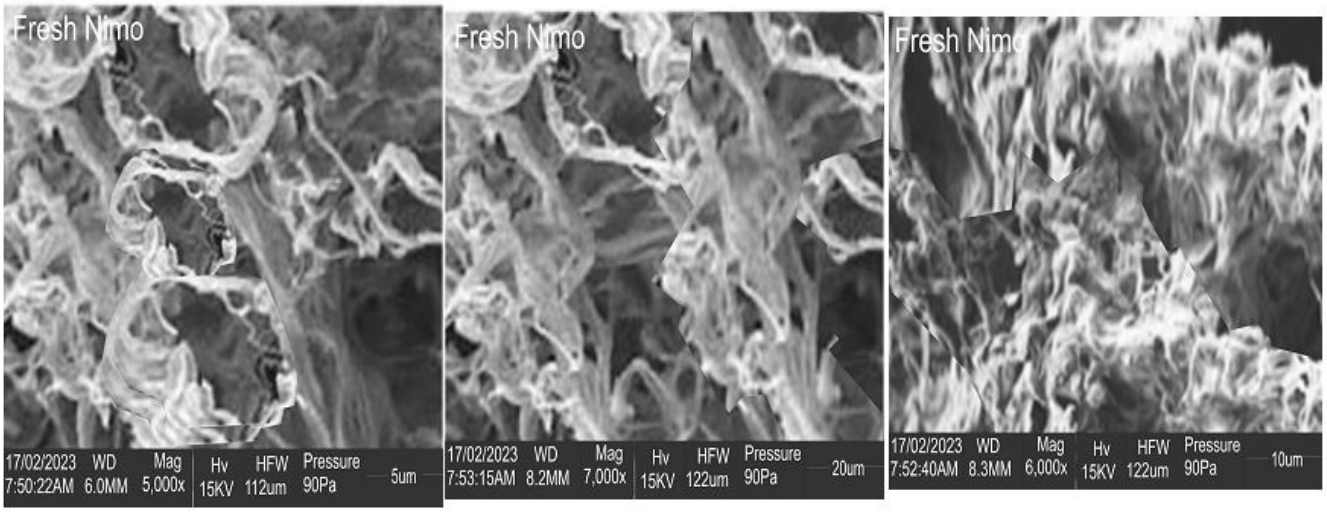

Figure 9.SEM image of fresh NiMo catalyst

The SEM micrograph of the fresh catalyst presented in Figure.9, shows the support surface that was modified after being exposed to the SEM. The carbon presence was confirmed by the elemental analysis, as shown in Figure 9 that indicates the presence of almost 4.5% carbon in the spent catalyst. Though different carbonaceous species were formed due to the reactive phase during the reaction, a carbon gasification at high temperature was expected and produced CO that had a higher syngas ratio. An SEM micrograph of NiMo particles is shown in Figure 9, which indicates the formation of porous-structure, block-shaped crystallites depicting the sintering of particles because of the higher temperature calcination.

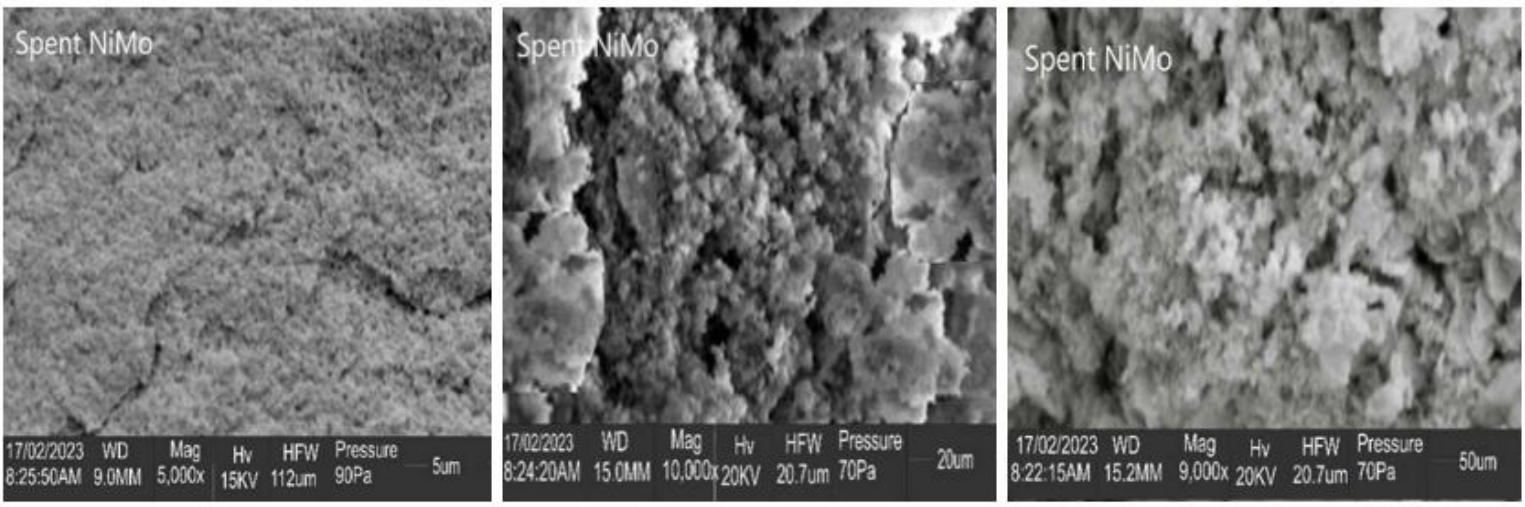

Figure 10.SEM image of spent NiMo catalyst

Sample was Ni- dominant whereas sample appeared to consist mainly of mixed-layer kaolin character with respect to the formamide test. Low magnification SEMs showed catalyst material with abundant pore space held together by a meshwork of clay coatings over relatively spentNiMo (Fig..10). The NiMo itself was composed of a crinkled mass of flat, platy particles, often with curled edges, about 1-2 μm diameter. There was abundant micro-pore space between the platy particles. The clay-rich nature of sample is evident from low magnification SEMs, the whole consisting of crinkled flakes and aggregates. The catalyst nature of sample is evident from low magnification SEMs, the whole consisting of crinkled flakes and aggregates arranged in sub- parallel fashion and with abundant void space. The constituent particles were mostly of an equant (in circles and having approximately equal diameters), platy shape, often bent or sinuous with curled edges, and ranged from ~0.5 to 2 μm diameter.

4. CONCLUSION

To address catalyst deactivation, particularly through carbon deposition, this study presents an in-depth thermal and structural analysis of fresh and spent NiMo catalysts using TGA, XRD, FTIR, and SEM techniques. Carbon deposition, the primary cause of catalyst deactivation, demands a detailed understanding of the mechanisms and types of carbonaceous materials formed. TGA results clearly delineate the stages of coke formation, identifying ‘medium’ and ‘hard’ coke as dominant species in the deactivated catalyst, with a consistent mass loss observed across varying heating rates. This uniformity in mass loss underscores the stability and potential regeneration challenges posed by carbon deposits, emphasizing the need for effective decoking strategies.XRD analysis reveals structural and compositional shifts, showing nickel and molybdenum in a stable spinel phase in fresh catalysts, with a transition to a rutile phase (tetragonal symmetry) in the spent sample. The presence of hexagonal-phase carbon in the spent NiMo suggests significant metallurgical restructuring due to carbon accumulation, which is crucial for understanding the durability and regeneration potential of the catalyst under harsh operational conditions. FTIR results further highlight the formation of new bonds in the spent catalyst, with peaks at 900 cm^{-1} (NiMo vibrations) and 744 cm^{-1} (O–C–O stretching) indicating an anatase structure. The evolution of these chemical bonds points to specific degradation pathways that affect the catalyst's activity, making it clear that mitigating these

changes could extend catalyst life. The SEM micrographs offer a visual depiction of the carbon deposition mechanisms and their morphological impact on the catalyst's surface. In the spent catalyst, the observed block-like crystallites and porous structures indicate sintering and particle aggregation due to high-temperature calcination, which not only hinders active site accessibility but also reduces overall catalytic efficiency. Understanding these morphological changes provides insight into the need for improved catalyst regeneration methods and temperature control strategies to minimize sintering and maintain catalyst performance. To enhance catalyst longevity, future studies should explore metallurgical modifications to NiMo composition that reduce carbon affinity or improve carbon resistance. Additionally, deeper analysis of carbon formation mechanisms via SEM and compositional shifts through XRD could identify structural modifications or protective coatings that resist coke formation, improving the robustness and sustainability of NiMo catalysts in heavy oil upgrading.

HIGHLIGHTS

- Experimental technique for coking of catalyst for optimization before characterization
- Methods to understand nature, position of coke and condition of spent catalyst
- Monitoring of decoking behavior to assess impact at different heating rates

Disclaimer (Artificial intelligence)

Author(s) hereby declare that NO generative AI technologies such as Large Language Models (ChatGPT, COPILOT, etc.) and text-to-image generators have been used during the writing or editing of this manuscript.

REFEREENCE

Argyle, M. D. and Bartholomew, C. H. (2015), "Heterogeneous catalyst deactivation and

regeneration: A review", *Catalysts*, 5(1), 145-269, doi: 10.3390/catal5010145

Asiedu, A., Davis, R. and Kumar, S. (2020), "Catalytic transfer hydrogenation and characterization of flash hydrolyzed microalgae into hydrocarbon fuels production (jet fuel)", *Fuel*, 261(2020), 116440, doi: 10.1016/j.fuel.2019.116440

Bare, S. R., Vila, F. D., Charochak, M. E., Prabhakar, S., Bradley, W. J., Jaye, C., Fischer, D. A and Rehr, J. J. (2017), "Characterization of coke on a Pt-Re/γ-Al2O3 re-forming catalyst: experimental and theoretical study", *ACS Catalysis*, 7 (2), 1452-1461, doi: 10.1021/acscatal.6b02785

Charisiou, N. L., Douvartzides, S. L., Siakavelas, G. I., Tzounis, L., Sebastian, V., Stolojan, V., Hinder, S. J. and Goula, M. A. (2019), "The relationship between reaction temperature and carbon deposition on Nickel catalysts based on Al2O3, ZrO2 or SiO2 supports during the biogas dry reforming reaction", *Catalysts*, 9(8), 676, doi: 10.3390/catal9080676

Chen, X., Ren. L., Yaseen, M., Wang, L., Liang, J., Liang, R. and Guo, H. (2019), "Synthesis, characterization and activity performance of Nickel-loaded spent FCC catalyst for pine gum hydrogenation", *RSC Advances 9(12)*, 6515-6525, doi: org/10.1039/C8RA07943A

Díaz, C. A., Garzón, W. F., Higuita, J. C. and Restrepo-Parra, E. (2018), "Characterization by TGA, SEM, and EDX of polymeric matrices used as cocaine camouflages", *Modern Applied Science 12(12)*, 119, doi: 10.5539/mas.v12n12p119

Dim, P., Hart, A., Wood, J., Macnaughtan, B. and Rigby, B. S. (2015), "Characterization of pore coking in catalyst for thermal down-hole upgrading of heavy oil", *Chemical Engineering Science, 131(1)*, 138–145, doi: 10.1016/j.ces.2015.03.052

Dim, P., Rigby, S., Hart, A. and Wood, J. (2014), "Optimization of coke resistant catalyst for thermal down-hole upgrading", *Chemical Engineering Science,* doi: org/10.2118/170070-MS

Dong C., Yin C., Wu T., Wu Z., Liu D. and Liu C. (2019), "Acid modification of the unsupported NiMo catalysts by Y-Zeolite nanoclusters", *Crystals*, 9(7), 344, doi: 10.3390/cryst9070344

Feng, R., Qiao, K., Wang, Y. and Yan, Z. (2013), "Perspective on FCC catalyst in China", *Applied Petrochemical Research*, 3(3) 63–70, doi: 10.1007/s13203-013-0030-1

Haridoss, S. (2017), "A study on role of catalyst used in catalytic cracking process in petroleum refining",*International Journal of ChemTech Research*, 10(7), 79-86, doi: 10.1021/acs.energyfuels.2c00567

Hart, A., Adam, M., Robinson, J.P., Rigby, S.P. and Wood, J. (2020), "Hydrogenation and dehydrogenation of Tetralin and Naphthalene to explore heavy oil upgrading using NiMo/Al2O3 and CoMo/Al2O3 catalysts heated with steel balls via induction, *Catalysts*, 10(5), 497, doi: 10.3390/catal10050497

Hart, A., Leeke, G., Greaves, M. and Wood, J. (2014), "Downhole Heavy Crude Oil Upgrading Using-CAPRI: Effect of Steam upon Upgrading and Coke Formation", *Energy & Fuels, 28(3)*, 1811-1819, doi: 10.1021/ef402300k

Ihediwa, C. (2021), "Fluid catalytic cracking", Kansa State University, retrieved from https://hdl.handle.net/2097/41695

Leyva, C., Ancheyta, J., Mariey, L., Travert, A. and Maugé, F. (2014), "Characterization study

of NiMo/SiO2-Al2O3 spent hydroprocessing catalysts for heavy oils", *Catalysis Today 220–222,* 89–96, doi: 10.1016/j.cattod.2013.10.007

Modekwe H.U., Mamo M.A., Moothi K. and Daramola M.O (2021), "Effect of different catalyst supports on the quality, yield and morphology of Carbon nanotubes produced from waste polypropylene plastics", *Catalysts*, 11(6), 692, doi: 10.3390/catal11060692

Mortezaeikia, V., Tavakoli, O. and Khodaparasti, M. S. (2021), "A review on kinetic study approach for pyrolysis of plastic wastes using thermogravimetric analysis", *Journal of Analytical and Applied Pyrolysis*, 160(1), 105340, doi: 10.1016/j.jaap.2021.105340

Nadeina, K. A., Budukva, S. V., Vatutina, Y. V., Mukhacheva, P. P., Gerasimov, E. Y., Pakharukova, V. P., limov, O. V. and Noskov, A. S (2022). "Unsupported Ni—Mo—W hydrotreating catalyst: influence of the atomic ratio of active metals on the HDS and HDN activity", 12(12),1671, *Catalysts*, 12(2)1671, doi: 10.3390/catal12121671

Nagar, N., Garg, H. and Gahan, C.S. (2021), "Characterization of different types of petroleum refinery spent catalyst followed by microbial mediated leaching of metal values", *Chem Rep*, 3(1),177-187, doi: 10.25082/CR.2021.01.002

Palos, R., Gutiérrez, A., Arandes, J. M. and Bilbao, J. (2018), "Catalyst used in fluid catalytic cracking (FCC) unit as a support of NiMo catalyst for light cycle oil hydroprocessing", *Fuel*, 216 (2018), 142–152, doi: 10.1016/j.fuel.2017.11.1486

Silvarrey, L. S. and Phan, A. N. (2016),"Kinetic study of municipal plastic waste", *International Journal of Hydrogen Energy*, 41(3), 16352-16364,doi: 10.1016/j.ijhydene.2016.05.202

Sundaram H. (2017), "A study on role of catalyst used in catalytic cracking process in petroleum refining", *International Journal of ChemTech Research, 10(7),* 79-86

Trueba, D., Palos, R., Bilbao, J., Arandes, J. M. and Gutiérrez, A. (2021), "Product composition and coke deposition in the hydrocracking of polystyrene blended with vacuum gasoil", *Fuel Processing Technology*, 224(2021) 107010, doi: 10.1016/j.fuproc.2021.107010

Zahran, A. I., Ahmed M.A., Wael, A. A., Mohamed, A. S., Huda, S. A. and Mohamed, A. M. (2020), "Enhancement of heavy vacuum gas oil desulfurization via using developed catalyst based on Al2O3", *Egyptian Journal of Chemistry, 63(10)*, 3801-3810, doi:10.21608/ejchem.2020.24452.2457

Zhang, Y. S., Lu, X., Owen, R. E., Manos, G., Xu, R., Wang, F. R. and Brett, R. D. (2019), "Fine Structural changes of fluid catalytic catalysts and characterization of coke formed resulting from heavy oil devolatilization", *Applied Catalysis B: Environmental*, 263:118329, doi: 10.1016/j.apcatb.2019.118329

Zhang, Y. S., Sun, G., Gao, S. and Xu, G. (2015),"Regeneration kinetics of Spent FCC catalyst via coke gasification in a micro fluidized bed", *Procedia Engineering*, 102(2015), 1758 – 1765, doi: 10.1016/j.proeng.2015.01.312